

UC Davis

UC Davis Previously Published Works

Title

Intermediate-Depth Earthquakes Controlled by Incoming Plate Hydration Along Bending-Related Faults

Permalink

<https://escholarship.org/uc/item/8kc932np>

Journal

Geophysical Research Letters, 46(7)

ISSN

0094-8276

Authors

Boneh, Yuval
Schottenfels, Emily
Kwong, Kevin
[et al.](#)

Publication Date

2019-04-16

DOI

10.1029/2018gl081585

Peer reviewed

1 **Intermediate depth earthquakes controlled by incoming plate hydration along**
2 **bending-related faults**

3 **Yuval Boneh^{1,2}, Emily Schottenfels³, Kevin Kwong⁴, Iris van Zelst⁵, Xinyue Tong⁶, Melody**
4 **Eimer⁷, Meghan S. Miller⁸, Louis Moresi⁹, Jessica M. Warren¹⁰, Douglas A. Wiens⁷, Magali**
5 **Billen¹¹, John Naliboff¹¹, Zhongwen Zhan¹²**

6 ¹ Department of Geological Sciences, Brown University, Providence, Rhode Island, USA

7 ² Now at Department of Geological and Environmental Sciences, Ben-Gurion University of the
8 Negev, Be'er-Sheva, Israel

9 ³ Department of Earth and Environment, Boston University, Boston, Massachusetts, USA

10 ⁴ Roy M. Huffington Department of Earth Science, Southern Methodist University, Dallas,
11 Texas, USA

12 ⁵ Seismology and Wave Physics, Institute of Geophysics, Department of Earth Sciences, ETH
13 Zürich, Zürich, Switzerland

14 ⁶ Department of Geological Sciences, Jackson School of Geosciences, University of Texas at
15 Austin, Austin, Texas, USA

16 ⁷ Department of Earth and Planetary Sciences, Washington University in St. Louis, Saint Louis,
17 Missouri, USA

18 ⁸ Research School of Earth Sciences, Australian National University, Canberra, Australia

19 ⁹ School of Earth Sciences, University of Melbourne, McCoy Building, Parkville, Australia

20 ¹⁰ Department of Geological Sciences, University of Delaware, Penny Hall, Newark, Delaware,
21 USA

22 ¹¹ Department of Geology, University of California, Davis, California, USA

23 ¹² Seismological Laboratory, Division of Geological and Planetary Sciences, California Institute
24 of Technology, Pasadena, California 91125, USA

25 Corresponding author: Yuval Boneh (bonehyuv@bgu.ac.il)

26 **Key Points:**

- 27 • Global survey demonstrates a correlation between bending faults in the incoming plate
28 and the seismicity rate of intermediate depth earthquakes
- 29 • Fault throw provides a proxy for overall fault damage and the ability of water to penetrate
30 and hydrate the incoming plate
- 31 • A mechanical parameter based on the incoming plate faulting controls the seismicity rate
32 of intermediate depth earthquakes
33

34 **Abstract**

35 Intermediate depth earthquakes (focal depths 70 – 300 km) are enigmatic with respect to their
36 nucleation and rupture mechanism, and the properties controlling their spatial distribution.
37 Several recent studies have shown a link between intermediate depth earthquakes and the
38 thermal-petrological path of subducting slabs in relation to the stability field of hydrous minerals.
39 Here we investigate whether the structural characteristics of incoming plates can be correlated
40 with the intermediate depth seismicity rate. We quantify the structural characteristics of 17
41 incoming plates by estimating the maximum fault throw (MFT) of bending-related faults. MFT
42 exhibits a statistically significant correlation with the seismicity rate. We suggest that the
43 correlation between fault throw and intermediate depth seismicity rate indicates the role of
44 hydration of the incoming plate, with larger faults reflecting increased damage, greater fluid
45 circulation, and thus more extensive slab hydration.

46 **Plain Language Summary**

47 In subduction zones, one tectonic plate plunges beneath another into the Earth's interior. Some
48 of the earthquakes that occur at subduction zones are unusual due to their occurrence at depths of
49 70 to 300 km ("intermediate depths"), deeper than the expected limit of brittle failure. In this
50 study, we evaluate whether the faults that form when a plate bends as it enters a subduction zone
51 can explain the occurrence of these deep earthquakes. Sea water penetrates deep into these faults
52 and forms new, hydrous minerals, but these new minerals are not stable deeper in the subduction
53 zone. Laboratory experiments show that breakdown of these hydrous minerals can cause
54 seismicity at depths of 70 – 300 km (intermediate depths). Here we examined a set of 17
55 subduction zone segments around the globe and found that the seismicity is correlated with the
56 faults that formed due to plate bending. This observation can be explained if the amount of
57 faulting prior to subduction controls the amount of hydrous mineral formation, which
58 subsequently determines the intensity and rate of subduction zone related intermediate depth
59 earthquakes.

60 **1 Introduction**

61 Intermediate depth earthquakes, defined as seismic events at depths of 70 – 300 km, are a
62 unique feature of subduction zones, delineating the upper crust and mantle of the subducting slab
63 in what is often referred to as the Wadati-Benioff zone [*Benioff, 1963; Wadati, 1928*]. The
64 dehydration of hydrous minerals in the subducted slab is the most commonly invoked
65 mechanism to explain events at these depths, where conditions of high temperature and pressure
66 should inhibit dynamic fracture or frictional sliding [*Green and Houston, 1995; Hirth and*
67 *Guillot, 2013; Meade and Jeanloz, 1991; Yamasaki and Seno, 2003*]. Rheological instabilities in
68 some hydrous minerals deformed under high pressures (> 1 GPa) have been observed
69 experimentally [*Ferrand et al., 2017; Jung et al., 2004; Jung et al., 2009; Okazaki and Hirth,*
70 *2016; Proctor and Hirth, 2016; Raleigh and Paterson, 1965*]. However, there is still ambiguity
71 regarding the specific mechanism(s) through which hydrous minerals can generate seismic
72 events. Additionally, there is considerable uncertainty about the degree of hydration of the
73 incoming plate, particularly for the oceanic upper mantle, which should be largely anhydrous due
74 to extraction of water during mid-ocean ridge melting [e.g., *Hacker, 2008*].

75 Extensional faulting due to plate bending provides a conduit for fluids into the crust and
76 uppermost mantle. Slab hydration and fluid circulation associated with plate bending-related

77 faults have been observed in seismic and electromagnetic studies [Cai *et al.*, 2018; Grevemeyer
78 *et al.*, 2007; Key *et al.*, 2012; Nedimović *et al.*, 2009; Van Avendonk *et al.*, 2011; Worzewski *et*
79 *al.*, 2011]. Numerical models suggest that stress and pressure changes during slab bending and
80 slab unbending can induce circulation of fluid through the fault zones into the lithospheric
81 mantle [Faccenda *et al.*, 2009; Faccenda *et al.*, 2012]. Subducting slabs have been inferred to
82 contain a significant amount of water, with hydration of the crust and mantle deduced from
83 seismic surveys [Abers, 2000; Cai *et al.*, 2018; Faccenda *et al.*, 2008; Peacock, 1990; Pozgay *et*
84 *al.*, 2009; Zhao *et al.*, 2007] and from chemical enrichments observed in arc magmas [e.g., Plank
85 and Langmuir, 1998; Stern, 2002].

86 This wide range of observations for incoming plate hydration, together with the
87 experimental evidence for embrittlement of hydrous minerals at high pressures, leads to an
88 expected relationship between incoming plate bending faults, amount of slab hydration, and
89 intermediate depth seismicity [Ranero *et al.*, 2005]. A correlation between the hydration state of
90 the incoming plate and the seismicity rate in the subducted slab has been established regionally
91 [Shillington *et al.*, 2015]. However, a previous attempt to find a worldwide relationship based on
92 the predicted water flux due to mineral dehydration did not find a correlation [Barcheck *et al.*,
93 2012]. Here, we show that incoming plate faults, which may control the extent of hydration
94 pathways in the subducted slab, correlates globally with the off-trench intermediate depth
95 earthquakes. We postulate that the global distribution of intermediate depth earthquakes is
96 controlled by the extent of faulting and fracturing on the incoming plate, and thus that hydration
97 is inherited through the brittle deformation history of the incoming plate.

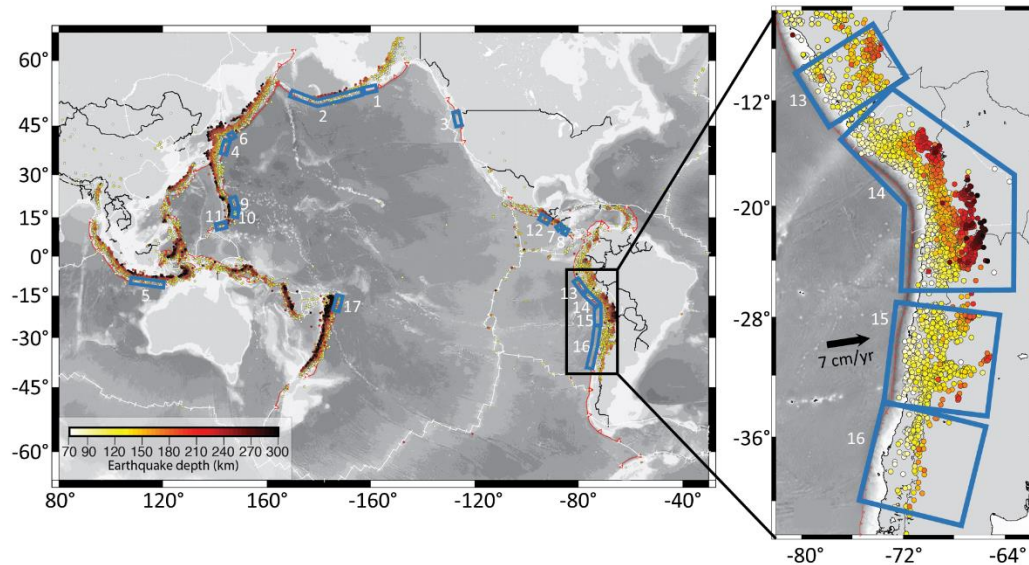
98 **2 Methods**

99 **2.1 Seismicity rate for intermediate depth earthquakes**

100 In order to quantify the seismic productivity of intermediate depth earthquakes, we used
101 the International Seismological Centre (ISC) Bulletin earthquake catalog (<http://www.isc.ac.uk>).
102 The ISC Bulletin is the most complete and comprehensive teleseismic earthquake catalog
103 available and includes documentation of globally recorded earthquake hypocenters, phases,
104 magnitudes, and other pertinent earthquake data [e.g., Di Giacomo *et al.*, 2015].

105 The intermediate depth events used in this study were chosen based on three criteria: (1)
106 focal depth of 70 – 300 km, (2) magnitude of $m_b \geq 4.5$, and (3) occurrence between 1964 to
107 2015. Although the ISC catalog contains events beginning in 1900, global monitoring of
108 earthquakes for these magnitudes became effective only in the 1960s. We define the seismicity
109 rate as the number of events normalized by the trench length (km) and time (year).

110 We estimated the seismicity rate for 17 subduction zone segments (Fig. 1) with trench
111 lengths of 210 – 1450 km (Table S1). For each segment, the increasing focal depth of
112 intermediate depth events away from the trench trace the descending slab. Maps of each
113 subduction zone showing the trench segments are provided in the supplementary material (Fig.
114 S1).



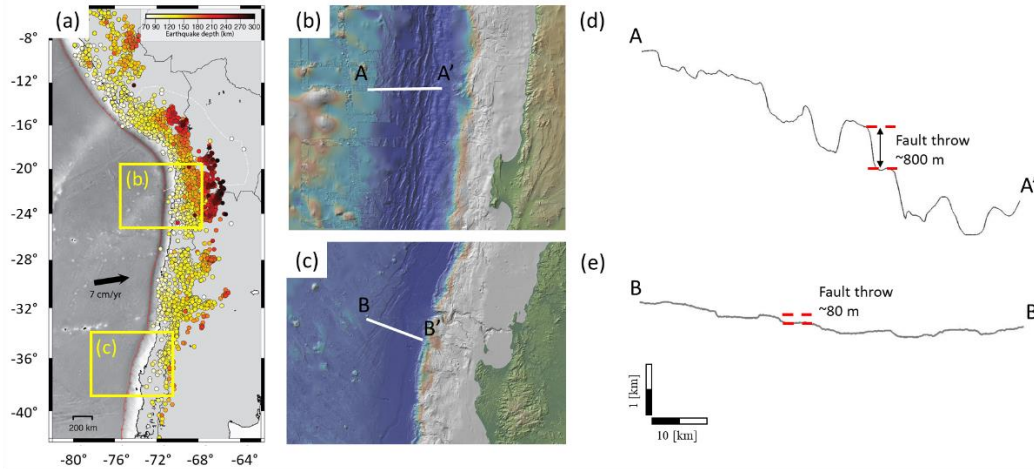
115

116 **Figure 1.** Left: Global map showing the subduction zone segments used in this paper (segment
 117 numbers correspond to IDs in Table S1). Intermediate depth earthquakes are delineated by
 118 circles colored by the hypocenter depth. Right: enlargement of the South-America trench,
 119 subdivided into 4 segments of different seismicity rates.

120 **2.2 Bending-related fault throw**

121 Slab flexure and the resulting tensional stresses generate normal faulting [e.g., Ludwig et
 122 al., 1966; Parsons and Molnar, 1976; Ranero et al., 2003]. The bending-related normal faults,
 123 manifested in horst and graben features, are a common characteristic of subduction zones and
 124 can be seen in seismic reflection images and bathymetric maps up to about 100 km seaward of
 125 the trench axis [e.g., Chapple and Forsyth, 1979; Hilde, 1983].

126 We quantified the vertical component of fault displacement (i.e., fault throw) in the
 127 incoming plate using a compilation of previously published bathymetry data from seismic
 128 reflection imaging and ship-based multibeam mapping [Table S2]. In regions with sparse or no
 129 data for bending fault offset, we used bathymetric data from the Global Multi-Resolution
 130 Topography (GMRT) [Ryan et al., 2009] accessed with GeoMapApp
 131 (<http://www.geomapapp.org/>). Topographic profiles orthogonal to both fault strike and the trench
 132 were manually selected and used to calculate the vertical fault throw on distinct seaward facing
 133 normal faults (Fig. 2 and Fig. S2). We quantified the maximum fault throw (MFT) for each
 134 region as a representation of the regional faulting intensity. Here we focus on MFT calculated as
 135 the average of the largest 10% of fault throw measurements for each region, but we also
 136 evaluated MFT based on the largest 5%, 20%, and 30% of fault throw measurements (Fig. S3).



137

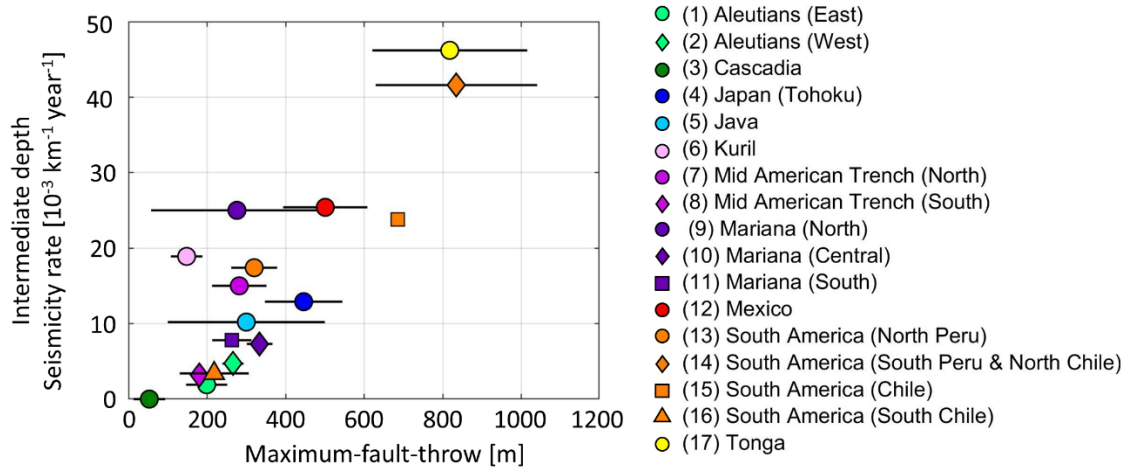
138 **Figure 2.** Bathymetry and incoming plate roughness due to bending faults. (a) The South-
 139 American coast with intermediate depth earthquakes (from Fig. 1). Yellow boxes show the
 140 locations of the zoomed-in bathymetry images shown in b and c. (b and c) Bathymetric maps
 141 (GRMT) where A-A' and B-B' indicate the cross sections d and e, respectively, showing the
 142 rough central (b) and conversely smooth southern (c) bathymetry off South America.

143 Fault throw represents fault displacement when a small variation in dip angle is assumed.
 144 We use it here to represent fault intensity on the assumption that this provides a proxy for
 145 hydration of the incoming plate. We therefore omit bathymetry related to seamounts and focus
 146 on bathymetry related to plate faulting. Topographic fault scarps and fault throw estimates have
 147 often been used to infer regional stress state, tectonics, and deformation rates where direct field
 148 studies are not possible, such as is in other submarine environments and planets [Schultz *et al.*,
 149 2006; Wilkins *et al.*, 2002].

150 3 Results

151 3.1 Comparison of incoming plate properties with seismicity rate

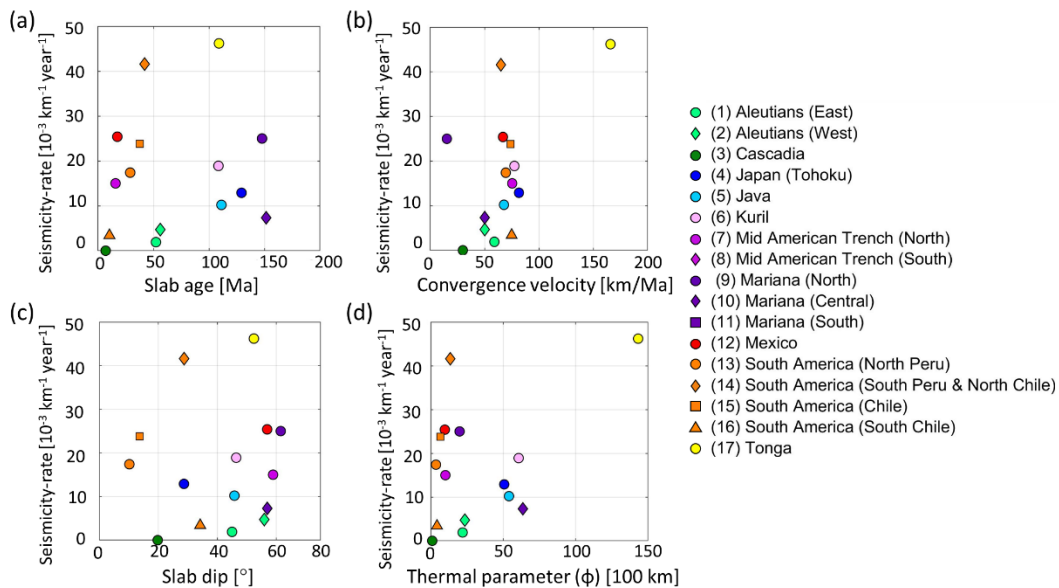
152 The co-variation of the bathymetric expression of faults (as represented by MFT), and the
 153 intermediate depth seismicity rate for the 17 trench segments is shown in Figure 3. This
 154 correlation suggests a general trend, where the largest fault throws are associated with an
 155 increase in intermediate depth seismicity. For example, the bathymetry of Cascadia presents low
 156 fault throw values of less than 50 m [Masson, 1991] and no intermediate depth earthquakes have
 157 been recorded at this subduction zone. On the other hand, the highly faulted slab at the Tonga
 158 trench has the highest seismicity rate of our dataset ($46.2 \cdot 10^{-3} \text{ km}^{-1} \text{ year}^{-1}$). Regional data show a
 159 similar trend. For example, we divided the Nazca plate, which subducts beneath South America,
 160 into four parts according to the bathymetric texture (Fig. 1). Along the northern part of the South
 161 America trench, the bathymetry is rough with MFT ~ 800 m, whereas the ocean-floor becomes
 162 smoother towards the south with MFT ~ 80 m (Fig. 2). The seismicity rate follows this trend,
 163 with higher seismicity rates corresponding to regions with rougher fault scarps. To test possible
 164 variations in the magnitude completeness of the ISC seismic catalog, we compared the seismicity
 165 rate with a threshold of $m_b \geq 4.5$ and threshold of $m_b \geq 5.6$ [Di Giacomo *et al.*, 2015]. We found
 166 no significant statistical difference in the seismicity rate between the two thresholds (Fig. S4).



167

168 **Figure 3.** The seismicity rate of intermediate depth earthquakes against the incoming plate
 169 maximum fault throw (MFT). MFT error bars are the standard deviation of the averaged 10%
 170 fraction largest fault throws, except Java, which is estimated to be 100 – 500 m by *Masson*
 171 [1991]. Error bars for segment 15 are smaller than the symbol size.

172 *Syracuse et al.* [2010] defined several slab properties and the correlation of these
 173 properties with seismicity rate is shown in Figure 4; slab age (Fig. 4a), convergence velocity
 174 (Fig. 4b), dip angle (Fig. 4c), and thermal parameter (Fig. 4d). In contrast to the positive trend
 175 between MFT and seismicity rate, none of these parameters show a clear correlation with
 176 intermediate depth earthquake intensity. In particular, the thermal parameter (ϕ), defined as the
 177 product of slab age and convergence velocity perpendicular to the trench [*Kirby et al.*, 1996],
 178 where higher values of ϕ correspond to cooler slabs. This parameter provides a proxy for slab
 179 temperature, assuming that heating of the subducting lithosphere is by conduction [*Molnar et al.*,
 180 1979]. The thermal state of a subduction zone has been assumed to control deep seismicity due
 181 to temperature-dependent mineral breakdowns reactions [*Kirby et al.*, 1991], yet ϕ is not
 182 correlated with seismicity rate (Fig. 4d).



183

184 **Figure 4.** The seismicity rate of intermediate depth earthquakes plotted against slab properties
185 from *Syracuse et al.*, [2010]: (a) age, (b) convergence velocity, (c) dip angle, and (d) thermal
186 parameter.

187 3.2 Statistical significance of the MFT correlation with seismicity rate

188 We use three different statistical measures to evaluate the correlations between MFT and
189 properties of the incoming plate (Table S3): (1) the Pearson product-moment correlation
190 coefficient, (2) the Kendall rank correlation coefficient, and (3) the Spearman rank correlation
191 coefficient. The Pearson's coefficient is used to explore the linear dependence between two
192 variables. The other two coefficients provide a measure of how well the relationship between the
193 two variables can be described by a monotonic function. In other words, they test the extent to
194 which the positive/negative relationship between two variables is systematic without the
195 necessity of a linear relationship. We also calculated the p-value to test the significance of the
196 correlations, where p varies between 0 and 1 and a small p-value indicates evidence against the
197 null hypothesis. In our analyses, the null hypothesis is that no correlation exists between the two
198 variables. We consider a correlation to be significant when $p \ll 0.05$ and the correlation
199 coefficients are higher than ~ 0.6 .

200 Our analysis reveals high, statistically significant correlations between seismicity rate and
201 MFT for all three statistical tests (Fig. S5). The correlation between seismicity rate and MFT
202 (average of the top 10% of fault throws) shows values of 0.86, 0.6 and 0.74 for the Pearson,
203 Kendall and Spearman coefficients, respectively (Table S3). In contrast, none of the four other
204 parameters (slab age, velocity, dip, and thermal parameter) show a significant correlation, with
205 coefficients < 0.54 , 0.21 , and 0.32 for the Pearson, Kendall and Spearman coefficients,
206 respectively (Fig. S4). We also tested different definitions for MFT, using both higher (20% and
207 30%) and lower (5%) percentages of the total fault throw to calculate MFT. The correlation of
208 seismicity rate with MFT is statistically significant for all definitions although using a higher
209 percentage (20 or 30% of the largest faults throws) results in slightly lower correlations.

210 The rank correlation coefficients (Kendall and Spearman) give slightly lower correlations
211 than the linear correlation coefficient (Pearson), because they are less sensitive to extreme
212 values. The high value of the Pearson coefficient partly stems from the high MFT and seismicity
213 rate values Tonga and South Peru-North Chile. Nevertheless, the fact that the rank dependence
214 coefficients also show significant correlations supports our finding of a positive relationship
215 between MFT and seismicity rate.

216 4 Discussion

217 Our results indicate that bending-related faulting of the incoming plate may be a
218 significant control on the seismicity rate of intermediate depth earthquakes. This relationship
219 between shallow incoming plate faults and intermediate depth seismicity rate was previously
220 shown for the Nazca and Cocos plates and was interpreted as fault reactivation [*Ranero et al.*,
221 2005]. However, *Warren et al.*, [2007, 2008] found that rupture directivity of intermediate depth
222 earthquakes was inconsistent with the orientation of outer-rise normal faults. Thus, the
223 correlation that we observe may instead be explained by hydration along these faults, with
224 subsequent embrittlement of the hydrated regions at >70 km, in accordance with nucleation
225 mechanisms for intermediate depth earthquakes.

226 4.1 Fault-zone damage leads to slab hydration

227 Bending faults provide a pathway for fluid circulation and deep hydration within the
228 downgoing plate [Emry and Wiens, 2015; Grevemeyer et al., 2007; Iyer et al., 2012; Key et al.,
229 2012; Nishikawa and Ide, 2015; Ranero and Sallares, 2004; Ranero et al., 2003; Tilmann et al.,
230 2008]. The damage associated with faulting leads to channels of increased permeability that
231 allow deep fluid penetration into the oceanic lithosphere [e.g., Naif et al., 2015] and these fluids
232 react with the host rock to form hydrous minerals [e.g., Andreani et al., 2007]. The ability of
233 fluids to penetrate and react deep in the lithosphere is governed by properties such as fracture
234 density, permeability, and porosity, which are enhanced by faulting [Sibson, 2000]. Importantly,
235 these physical properties are expected to evolve through progressive displacement on faults.

236 Fault displacement and length scaling relationships [Cowie and Scholz, 1992; Schultz et
237 al., 2006] suggest that for greater fault displacement (and therefore greater fault throw), a larger
238 volume of the incoming plate is damaged. This provides the potential for enhanced hydration on
239 larger faults and thus more hydrous minerals would then be available at intermediate depths to
240 cause dehydration embrittlement. Gouge thickness [Scholz, 1987] and damage zone thickness
241 [Faulkner et al., 2011; Savage and Brodsky, 2011; Shipton and Cowie, 2001] increase with
242 increased fault displacement. Hence, the ability of fluids to migrate through the rock is
243 dependent on the damage-zone structure. Within the core of a fault, the permeability may be low
244 due to the presence of fault gouge. However, in material adjacent to the fault core, the
245 permeability can be an order of magnitude higher as a result of cracking in the region known as
246 the damage-zone [Caine et al., 1996; Evans et al., 1997].

247 Mitchell and Faulkner [2012] showed that fracture density, damage-zone width, and
248 fault displacement control overall damage zone permeability and that fault-related fracturing and
249 permeability scale with fault displacement. The displacement (d) is scaled with the width of
250 damage surrounding the fault (DW):

$$251 \quad DW = \frac{a d}{b+d} \quad (1)$$

252 where DW is in meters, and a and b are constants with values of 96.25 and 147.16,
253 respectively [Mitchell and Faulkner, 2012; Savage and Brodsky, 2011] based on regression of
254 fault-zone data [Faulkner et al., 2011]. Cowie and Scholz [1992] showed that the fault length (L)
255 can be scaled with the displacement:

$$256 \quad d/L \propto 0.01 \quad (2)$$

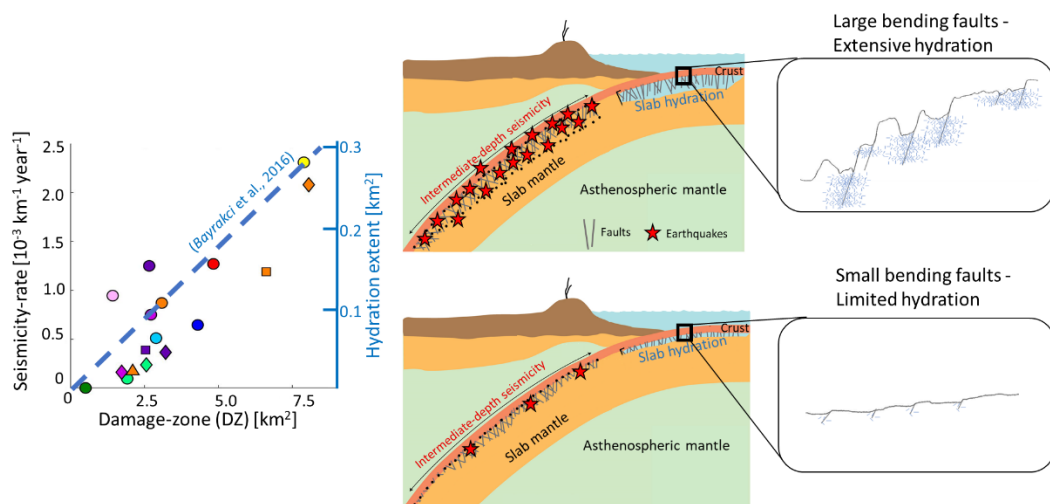
257 Assuming Andersonian faults with 60° dip, displacement can be estimated from the fault
258 throw. Using equations 1 and 2, the area of the damage-zone (DZ) due to faulting can be
259 estimated:

$$260 \quad DZ = L \cdot DW \quad (3)$$

261 where DZ has units of m^2 . The damage-zone associated with faulting increases the
262 permeability around the fault and allows fluid infiltration and subsequent hydration [Reynolds
263 and Lister, 1987; Rüpke and Hasenclever, 2017].

264 For the bending-faults in this study, the damage-zone width, estimated from the fault-
265 throw, shows a quasi-linear relationship with the seismicity rate (Figure 5). As hydration kinetics
266 are relatively fast [Martin and Fyfe, 1970], the limiting factor for slab hydration is the supply of
267 water through brittle slab fractures and faults [Rüpke et al., 2013]. Although mineral production
268 during hydration reactions has the potential to seal cracks [e.g., Michibayashi, et al., 2008], the

269 reaction also results in a positive volume change that can generate additional fracturing and
 270 permeability [Audet et al., 2009; Jamtveit et al., 2009]. The relationship between mechanical
 271 faulting and the extent of plate hydration has been observed in extensional faults at continental
 272 rifts [Pérez-Gussinyé and Reston, 2001], where faults have been found to serve as fluid conduits
 273 for hydration. Bayrakci et al. [2016] used seismic tomography of a continental margin offshore
 274 from western Spain to determine that the volume of serpentine had a linear dependence with the
 275 amount of fault displacement, consistent with the linear relationship presented in this study (Fig.
 276 5). We conclude that fault displacement controls the overall damage zone structure and
 277 permeability of the subducted plate and that bending faults function as conduits for fluid
 278 infiltration into the oceanic lithosphere. Therefore, maximum fault throw provides a proxy for
 279 the extent of hydration in the slab, which later leads to intermediate depth seismicity.



280
 281 **Figure 5.** Left: seismicity rate plotted against damage-zone width estimated from fault
 282 displacements. Data from this study show a similar relationship to the estimated extent of
 283 hydration as a function of damage-zone width as determined from seismic data by Bayrakci et al.
 284 [2016] for the Iberia rifted margin. Right: schematic diagram of a subduction zone, illustrating
 285 the relationship between bending faulting, incoming plate hydration, and intermediate depth
 286 seismicity (modified from Billen [2009]).

287 4.2 The effect of incoming plate structure on intermediate depth earthquakes

288 Previous studies have investigated the relationship between the thermal structure of the
 289 slab, dehydration, and intermediate depth seismicity [Abers et al., 2013; Hacker et al., 2003; van
 290 Keken et al., 2011; Wei et al., 2017]. The premise behind such studies is that dehydration and
 291 breakdown of hydrous minerals cause intermediate depth seismicity, as the thermo-petrological
 292 state of the slab determines when mineral phase boundaries are crossed, controlling the depth of
 293 earthquakes [Gorbatov and Kostoglodov, 1997; Hacker et al., 2003; Peacock, 2001]. Fracturing,
 294 elevated fluid pressure, and stress heterogeneities due to dehydration may all contribute to the
 295 nucleation of intermediate depth earthquakes [Davies, 1999; Ferrand et al., 2017; Gasc et al.,
 296 2017].

297 The correlation of thermal structure and slab age with intermediate depth seismicity
 298 suggests that the nucleation mechanism is temperature dependent [Brudzinski et al., 2007]. This

299 could be associated with the specific rheology of the hydrous minerals that have formed due to
300 the brittle-ductile-brittle transitions characteristic of many hydrous minerals [Brantut *et al.*,
301 2011; Jung *et al.*, 2009; Proctor and Hirth, 2016; Raleigh and Paterson, 1965]. Alternatively,
302 seismicity may result from dehydration embrittlement and the related change of fluid pressure
303 and stress heterogeneities [Ferrand *et al.*, 2017; Hirth and Guillot, 2013; Okazaki and Hirth,
304 2016]. Although the pressure-temperature conditions in the slab are a first-order control on the
305 release of fluids at intermediate depths, here we find that a mechanical parameter, fault throw,
306 determines the net availability of fluids and therefore controls the intensity of intermediate depth
307 seismicity.

308 **5 Conclusions**

309 We show a significant correlation between a global dataset of intermediate depth
310 seismicity rates and the occurrence of shallow faulting caused by plate bending. Other
311 parameters of the subducted slab such as plate age, convergence velocity, dip angle, and thermal
312 parameter do not show a statistically significant correlation. Our results suggest that shallow
313 processes associated with bending faults of the incoming plate have a strong control over
314 intermediate depth seismicity rate. We propose that the hydration extent of the subducted slab,
315 estimated from its faulting, exerts a primary control on the prevalence of intermediate depth
316 seismicity. Thermo-petrological models that seek to describe intermediate depth earthquakes
317 through mineral phase stability and breakdown of hydrous phases should also account for the
318 extent of hydration within the slab.

319 **Acknowledgments**

320 This research project was initiated at the 2017 Cooperative Institute for Dynamic Earth Research
321 (CIDER) summer program "Subduction Zone Dynamics" at the University of California,
322 Berkeley. We wish to thank the other organizers B. Romanowicz, P. van Keken, E. Hauri, and C.
323 Till. CIDER-II is funded as a "Synthesis Center" by the Frontiers of Earth Systems Dynamics
324 (FESD) program of NSF under grant number EAR-1135452. We also wish to thank Geoffrey
325 Abers and an anonymous reviewer for constructive comments and gratefully acknowledge Yi
326 Hu, Wang-Ping Chen, Samer Naif, and Hannah Rabinowitz for valuable discussions. Bathymetry
327 profiles from GeoMapApp (<http://www.geomapapp.org/>) were used in this study and are
328 included in the supporting information. A bathymetry profile from the Mariana trench (center)
329 was collected by R/V Langseth cruise, MGL1204 and is available from NOAA at
330 <http://www.marine-geo.org/link/entry.php?id=MGL1204>. Seismic data for the Japan trench was
331 collected by JAMSTEC (KR13-11). Seismicity data used to quantify the intermediate depth
332 seismicity rate was taken from the International Seismological Centre (ISC) Bulletin earthquake
333 catalog (<http://www.isc.ac.uk>).

334

335 **References**

- 336 Abers, G.A., 2000. Hydrated subducted crust at 100–250 km depth. *Earth and Planetary Science*
337 *Letters*, 176(3-4), pp.323-330.
- 338 Abers, G. A., J. Nakajima, P. E. van Keken, S. Kita, and B. R. Hacker (2013), Thermal–
339 petrological controls on the location of earthquakes within subducting plates, *Earth and*
340 *Planetary Science Letters*, 369, 178-187.

- 341 Andreani, M., C. Mével, A. M. Boullier, and J. Escartin (2007), Dynamic control on serpentine
342 crystallization in veins: Constraints on hydration processes in oceanic peridotites,
343 *Geochemistry, Geophysics, Geosystems*, 8(2).
- 344 Barcheck, C. G., D. A. Wiens, P. E. van Keken, and B. R. Hacker (2012), The relationship of
345 intermediate-and deep-focus seismicity to the hydration and dehydration of subducting slabs,
346 *Earth and Planetary Science Letters*, 349, 153-160.
- 347 Bayrakci, G., T. Minshull, D. Sawyer, T. J. Reston, D. Klaeschen, C. Papenberg, C. R. Ranero, J.
348 Bull, R. Davy, and D. Shillington (2016), Fault-controlled hydration of the upper mantle
349 during continental rifting, *Nature Geoscience*, 9(5), 384.
- 350 Benioff, H. (1963), Source wave forms of three earthquakes, *Bulletin of the Seismological*
351 *Society of America*, 53(5), 893-903.
- 352 Bilek, S. L., S. Y. Schwartz, and H. R. DeShon (2003), Control of seafloor roughness on
353 earthquake rupture behavior, *Geology*, 31(5), 455-458.
- 354 Billen, M. I. (2009), Tectonics: Soaking slabs, *Nature Geoscience*, 2(11), 744.
- 355 Billen, M.I. and Gurnis, M., 2005. Constraints on subducting plate strength within the Kermadec
356 trench. *Journal of Geophysical Research: Solid Earth*, 110(B5).
- 357 Bondár, I., and D. Storchak (2011), Improved location procedures at the International
358 Seismological Centre, *Geophysical Journal International*, 186(3), 1220-1244.
- 359 Bondár, I., E. R. Engdahl, A. Villaseñor, J. Harris, and D. Storchak (2015), ISC-GEM: Global
360 instrumental earthquake catalogue (1900–2009), II. Location and seismicity patterns, *Physics*
361 *of the Earth and Planetary Interiors*, 239, 2-13.
- 362 Boston, B., G. F. Moore, Y. Nakamura, and S. Kodaira (2014), Outer-rise normal fault
363 development and influence on near-trench décollement propagation along the Japan Trench,
364 off Tohoku, *Earth, Planets and Space*, 66(1), 135.
- 365 Bouchon, M., D. Marsan, V. Durand, M. Campillo, H. Perfettini, R. Madariaga, and B. Gardonio
366 (2016), Potential slab deformation and plunge prior to the Tohoku, Iquique and Maule
367 earthquakes, *Nature Geoscience*, 9(5), 380.
- 368 Brantut, N., A. Schubnel, and Y. Guéguen (2011), Damage and rupture dynamics at the brittle-
369 ductile transition: The case of gypsum, *Journal of Geophysical Research: Solid Earth*,
370 116(B1).
- 371 Brudzinski, M. R., C. H. Thurber, B. R. Hacker, and E. R. Engdahl (2007), Global prevalence of
372 double Benioff zones, *Science*, 316(5830), 1472-1474.
- 373 Cai, C., D. A. Wiens, W. Shen, and M. Eimer (2018), Water input into the Mariana subduction
374 zone estimated from ocean-bottom seismic data, *Nature*, 563(7731), 389.
- 375 Caine, J. S., J. P. Evans, and C. B. Forster (1996), Fault zone architecture and permeability
376 structure, *Geology*, 24(11), 1025-1028.
- 377 Chapple, W. M., and D. W. Forsyth (1979), Earthquakes and bending of plates at trenches,
378 *Journal of Geophysical Research: Solid Earth*, 84(B12), 6729-6749.
- 379 Centre, I. S. (2015), On-line Bulletin.

380 Cowie, P. A., and C. H. Scholz (1992), Displacement-length scaling relationship for faults: data
381 synthesis and discussion, *Journal of Structural Geology*, 14(10), 1149-1156.

382 Davies, J. H. (1999), The role of hydraulic fractures and intermediate depth earthquakes in
383 generating subduction zone magmatism, *Nature*, 398(6723), 142.

384 Di Giacomo, D., I. Bondár, D. A. Storchak, E. R. Engdahl, P. Bormann, and J. Harris (2015),
385 ISC-GEM: Global Instrumental Earthquake Catalogue (1900–2009), III. Re-computed MS
386 and mb, proxy MW, final magnitude composition and completeness assessment, *Physics of
387 the Earth and Planetary Interiors*, 239, 33-47.

388 Emry, E. L., and D. A. Wiens (2015), Incoming plate faulting in the Northern and Western
389 Pacific and implications for subduction zone water budgets, *Earth and Planetary Science
390 Letters*, 414, 176-186.

391 Evans, J. P., C. B. Forster, and J. V. Goddard (1997), Permeability of fault-related rocks, and
392 implications for hydraulic structure of fault zones, *Journal of Structural Geology*, 19(11),
393 1393-1404.

394 Faccenna, C., Holt, A.F., Becker, T.W., Lallemand, S. and Royden, L.H., 2018. Dynamics of the
395 Ryukyu/Izu-Bonin-Marianas double subduction system. *Tectonophysics*, 746, pp.229-238.

396 Faccenda, M., T. V. Gerya, and L. Burlini (2009), Deep slab hydration induced by bending-
397 related variations in tectonic pressure, *Nature Geoscience*, 2(11), 790-793.

398 Faccenda, M., L. Burlini, T. V. Gerya, and D. Mainprice (2008), Fault-induced seismic
399 anisotropy by hydration in subducting oceanic plates, *Nature*, 455(7216), 1097.

400 Faccenda, M., T. V. Gerya, N. S. Mancktelow, and L. Moresi (2012), Fluid flow during slab
401 unbending and dehydration: Implications for intermediate-depth seismicity, slab weakening
402 and deep water recycling, *Geochemistry, Geophysics, Geosystems*, 13(1).

403 Faulkner, D., T. Mitchell, E. Jensen, and J. Cembrano (2011), Scaling of fault damage zones
404 with displacement and the implications for fault growth processes, *Journal of Geophysical
405 Research: Solid Earth*, 116(B5).

406 Ferrand, T. P., N. Hilaret, S. Incel, D. Deldicque, L. Labrousse, J. Gasc, J. Renner, Y. Wang, H.
407 W. Green II, and A. Schubnel (2017), Dehydration-driven stress transfer triggers
408 intermediate depth earthquakes, *Nature communications*, 8, 15247.

409 Gasc, J., N. Hilaret, T. Yu, T. Ferrand, A. Schubnel, and Y. Wang (2017), Faulting of natural
410 serpentinite: Implications for intermediate depth seismicity, *Earth and Planetary Science
411 Letters*, 474, 138-147.

412 Gorbatov, A., and V. Kostoglodov (1997), Maximum depth of seismicity and thermal parameter
413 of the subducting slab: general empirical relation and its application, *Tectonophysics*, 277(1-
414 3), 165-187.

415 Green, H. W., and H. Houston (1995), The mechanics of deep earthquakes, *Annual Review of
416 Earth and Planetary Sciences*, 23(1), 169-213.

417 Grevemeyer, I., C. R. Ranero, E. R. Flueh, D. Kläschen, and J. Bialas (2007), Passive and active
418 seismological study of bending-related faulting and mantle serpentinization at the Middle
419 America trench, *Earth and Planetary Science Letters*, 258(3-4), 528-542.

- 420 Hacker, B. R. (2008), H₂O subduction beyond arcs, *Geochemistry, Geophysics, Geosystems*,
421 9(3).
- 422 Hacker, B. R., S. M. Peacock, G. A. Abers, and S. D. Holloway (2003), Subduction factory 2.
423 Are intermediate-depth earthquakes in subducting slabs linked to metamorphic dehydration
424 reactions?, *Journal of Geophysical Research: Solid Earth*, 108(B1).
- 425 Han, S., S. M. Carbotte, J. P. Canales, M. R. Nedimović, H. Carton, J. C. Gibson, and G. W.
426 Horning (2016), Seismic reflection imaging of the Juan de Fuca plate from ridge to trench:
427 New constraints on the distribution of faulting and evolution of the crust prior to subduction,
428 *Journal of Geophysical Research: Solid Earth*, 121(3), 1849-1872.
- 429 Hilde, T. W. (1983), Sediment subduction versus accretion around the Pacific, *Tectonophysics*,
430 99(2-4), 381-397.
- 431 Hirth, G., and S. Guillot (2013), Rheology and tectonic significance of serpentinite, *Elements*,
432 9(2), 107-113.
- 433 Iyer, K., L. H. Rüpke, J. Phipps Morgan, and I. Grevemeyer (2012), Controls of faulting and
434 reaction kinetics on serpentinitization and double Benioff zones, *Geochemistry, Geophysics,*
435 *Geosystems*, 13(9).
- 436 Jamtveit, B., C. V. Putnis, and A. Malthe-Sørensen (2009), Reaction induced fracturing during
437 replacement processes, *Contributions to Mineralogy and Petrology*, 157(1), 127-133.
- 438 Jung, H., H. W. Green II, and L. F. Dobrzhinetskaya (2004), Intermediate depth earthquake
439 faulting by dehydration embrittlement with negative volume change, *Nature*, 428(6982),
440 545-549.
- 441 Jung, H., Y. Fei, P. G. Silver, and H. W. Green (2009), Frictional sliding in serpentine at very
442 high pressure, *Earth and Planetary Science Letters*, 277(1), 273-279.
- 443 Key, K., S. Constable, T. Matsuno, R. L. Evans, and D. Myer (2012), Electromagnetic detection
444 of plate hydration due to bending faults at the Middle America Trench, *Earth and Planetary*
445 *Science Letters*, 351, 45-53.
- 446 Kimura, G., Y. Hashimoto, Y. Kitamura, A. Yamaguchi, and H. Koge (2014), Middle Miocene
447 swift migration of the TTT triple junction and rapid crustal growth in southwest Japan: A
448 review, *Tectonics*, 33(7), 1219-1238.
- 449 Kirby, S. H., W. B. Durham, and L. A. Stern (1991), Mantle phase changes and deep-earthquake
450 faulting in subducting lithosphere, *Science*, 252(5003), 216-225.
- 451 Kirby, S.H., S. Stein, E.A. Okal, and D.C. Rubie (1996), Metastable mantle phase
452 transformations and deep earthquakes in subducting oceanic lithosphere. *Reviews of*
453 *geophysics*, 34(2), pp.261-306.
- 454 Ludwig, W.J., J.I. Ewing, M. Ewing, S. Murauchi, N. Den, S. Asano, H. Hotta, M. Hayakawa, T.
455 Asanuma, K. Ichikawa, and I. Noguchi (1966), Sediments and structure of the Japan Trench.
456 *Journal of Geophysical Research*, 71(8), pp.2121-2137
- 457 Martin, B., and W. Fyfe (1970), Some experimental and theoretical observations on the kinetics
458 of hydration reactions with particular reference to serpentinitization, *Chemical geology*, 6,
459 185-202.

- 460 Massell, C. G. (2002), *Large-scale structural variation of trench outer slopes and rises.*
- 461 Masson, D. (1991), Fault patterns at outer trench walls, *Marine Geophysical Researches*, 13(3),
462 209-225.
- 463 Meade, C., and R. Jeanloz (1991), Deep-focus earthquakes and recycling of water into the
464 Earth's mantle, *Science*, 252(5002), 68-72.
- 465 Michibayashi, K., Hirose, T., Nozaka, T., Harigane, Y., Escartin, J., Delius, H., Linek, M. and
466 Ohara, Y., 2008. Hydration due to high-T brittle failure within in situ oceanic crust, 30 N
467 Mid-Atlantic Ridge. *Earth and Planetary Science Letters*, 275(3), pp.348-354.
- 468 Miller, M.S., Gorbatov, A. and Kennett, B.L.N., 2005. Heterogeneity within the subducting
469 Pacific slab beneath the Izu–Bonin–Mariana arc: Evidence from tomography using 3D ray
470 tracing inversion techniques. *Earth and Planetary Science Letters*, 235(1-2), pp.331-342.
- 471 Mitchell, T., and D. Faulkner (2012), Towards quantifying the matrix permeability of fault
472 damage zones in low porosity rocks, *Earth and Planetary Science Letters*, 339, 24-31.
- 473 Molnar, P., D. Freedman, and J. S. Shih (1979), Lengths of intermediate and deep seismic zones
474 and temperatures in downgoing slabs of lithosphere, *Geophysical Journal International*,
475 56(1), 41-54.
- 476 Nakamura, Y., Kodaira, S., Cook, B.J., Jeppson, T., Kasaya, T., Yamamoto, Y., Hashimoto, Y.,
477 Yamaguchi, M., Obana, K. and Fujie, G., 2014. Seismic imaging and velocity structure
478 around the JFAST drill site in the Japan Trench: low V_p , high V_p/V_s in the transparent
479 frontal prism. *Earth, Planets and Space*, 66(1), p.121.
- 480 Naliboff, J. B., M. I. Billen, T. Gerya, and J. Saunders (2013), Dynamics of outer-rise faulting in
481 oceanic-continental subduction systems, *Geochemistry, Geophysics, Geosystems*, 14(7),
482 2310-2327.
- 483 Naif, S., K. Key, S. Constable, and R. L. Evans (2015), Water-rich bending faults at the Middle
484 America Trench, *Geochemistry, Geophysics, Geosystems*, 16(8), 2582-2597.
- 485 Nedimović, M. R., D. R. Bohnenstiehl, S. M. Carbotte, J. P. Canales, and R. P. Dziak (2009),
486 Faulting and hydration of the Juan de Fuca plate system, *Earth and Planetary Science
487 Letters*, 284(1-2), 94-102.
- 488 Nishikawa, T., and S. Ide (2015), Background seismicity rate at subduction zones linked to slab-
489 bending-related hydration, *Geophysical Research Letters*, 42(17), 7081-7089.
- 490 Okazaki, K., and G. Hirth (2016), Dehydration of lawsonite could directly trigger earthquakes in
491 subducting oceanic crust, *Nature*, 530(7588), 81-84.
- 492 Parsons, B. and P. Molnar (1976). The origin of outer topographic rises associated with trenches.
493 *Geophysical Journal International*, 45(3), pp.707-712.
- 494 Peacock, S. M. (2001), Are the lower planes of double seismic zones caused by serpentine
495 dehydration in subducting oceanic mantle?, *Geology*, 29(4), 299-302.
- 496 Pérez-Gussinyé, M., and T. J. Reston (2001), Rheological evolution during extension at
497 nonvolcanic rifted margins: onset of serpentization and development of detachments
498 leading to continental breakup, *Journal of Geophysical Research: Solid Earth*, 106(B3),
499 3961-3975.

500 Plank, T. and Langmuir, C.H., 1998. The chemical composition of subducting sediment and its
501 consequences for the crust and mantle. *Chemical geology*, 145(3), pp.325-394.

502 Pozgay, S. H., D. A. Wiens, J. A. Conder, H. Shiobara, and H. Sugioka (2009), Seismic
503 attenuation tomography of the Mariana subduction system: Implications for thermal
504 structure, volatile distribution, and slow spreading dynamics, *Geochemistry, Geophysics,*
505 *Geosystems*, 10(4).

506 Proctor, B., and G. Hirth (2016), “Ductile to brittle” transition in thermally stable antigorite
507 gouge at mantle pressures, *Journal of Geophysical Research: Solid Earth*, 121(3), 1652-
508 1663.

509 Raleigh, C., and M. Paterson (1965), Experimental deformation of serpentinite and its tectonic
510 implications, *Journal of Geophysical Research*, 70(16), 3965-3985.

511 Ranero, C. R., and V. Sallares (2004), Geophysical evidence for hydration of the crust and
512 mantle of the Nazca plate during bending at the north Chile trench, *Geology*, 32(7), 549-552.

513 Ranero, C. R., J. P. Morgan, K. McIntosh, and C. Reichert (2003), Bending-related faulting and
514 mantle serpentinitization at the Middle America trench, *Nature*, 425(6956), 367.

515 Ranero, C. R., A. Villaseñor, J. Phipps Morgan, and W. Weinrebe (2005), Relationship between
516 bend-faulting at trenches and intermediate-depth seismicity, *Geochemistry, Geophysics,*
517 *Geosystems*, 6(12).

518 Reynolds, S. J., and G. S. Lister (1987), Structural aspects of fluid-rock interactions in
519 detachment zones, *Geology*, 15(4), 362-366.

520 Rüpke, L. H., and J. Hasenclever (2017), Global rates of mantle serpentinitization and H₂
521 production at oceanic transform faults in 3-D geodynamic models, *Geophysical Research*
522 *Letters*, 44(13), 6726-6734.

523 Rüpke, L. H., D. W. Schmid, M. Perez-Gussinye, and E. Hartz (2013), Interrelation between
524 rifting, faulting, sedimentation, and mantle serpentinitization during continental margin
525 formation—including examples from the Norwegian Sea, *Geochemistry, Geophysics,*
526 *Geosystems*, 14(10), 4351-4369.

527 Ryan, W.B., Carbotte, S.M., Coplan, J.O., O'Hara, S., Melkonian, A., Arko, R., Weissel, R.A.,
528 Ferrini, V., Goodwillie, A., Nitsche, F. and Bonczkowski, J., 2009. Global multi-resolution
529 topography synthesis. *Geochemistry, Geophysics, Geosystems*, 10(3).

530 Ryan, W. B., S. M. Carbotte, J. O. Coplan, S. O'Hara, A. Melkonian, R. Arko, R. A. Weissel, V.
531 Ferrini, A. Goodwillie, and F. Nitsche (2009), Global multi-resolution topography synthesis,
532 *Geochemistry, Geophysics, Geosystems*, 10(3).

533 Savage, H. M., and E. E. Brodsky (2011), Collateral damage: Evolution with displacement of
534 fracture distribution and secondary fault strands in fault damage zones, *Journal of*
535 *Geophysical Research: Solid Earth*, 116(B3).

536 Scholz, C. H. (1987), Wear and gouge formation in brittle faulting, *Geology*, 15(6), 493-495.

537 Schultz, R. A., C. H. Okubo, and S. J. Wilkins (2006), Displacement-length scaling relations for
538 faults on the terrestrial planets, *Journal of Structural Geology*, 28(12), 2182-2193.

539 Shillington, D. J., A. Bécel, M. R. Nedimović, H. Kuehn, S. C. Webb, G. A. Abers, K. M.
540 Keranen, J. Li, M. Delescluse, and G. A. Mattei-Salicrup (2015), Link between plate fabric,
541 hydration and subduction zone seismicity in Alaska, *Nature Geoscience*, 8(12), 961.

542 Shipton, Z., and P. Cowie (2001), Damage zone and slip-surface evolution over μm to km scales
543 in high-porosity Navajo sandstone, Utah, *Journal of Structural Geology*, 23(12), 1825-1844.

544 Sibson, R. H. (2000), Fluid involvement in normal faulting, *Journal of Geodynamics*, 29(3-5),
545 469-499.

546 Stern, R. J. (2002), Subduction zones, *Reviews of geophysics*, 40(4).

547 Syracuse, E. M., P. E. van Keken, and G. A. Abers (2010), The global range of subduction zone
548 thermal models, *Physics of the Earth and Planetary Interiors*, 183(1), 73-90.

549 Tilmann, F. J., I. Grevemeyer, E. R. Flueh, T. Dahm, and J. Göbner (2008), Seismicity in the
550 outer rise offshore southern Chile: indication of fluid effects in crust and mantle, *Earth and*
551 *Planetary Science Letters*, 269(1-2), 41-55.

552 Uyeda, S., and Z. Ben-Avraham (1972), Origin and development of the Philippine Sea, *Nature*
553 *Physical Science*, 240(104), 176.

554 Van Avendonk, H. J., W. S. Holbrook, D. Lizarralde, and P. Denyer (2011), Structure and
555 serpentinization of the subducting Cocos plate offshore Nicaragua and Costa Rica,
556 *Geochemistry, Geophysics, Geosystems*, 12(6).

557 Van der Hilst, R., S. Widiyantoro, and E. Engdahl (1997), Evidence for deep mantle circulation
558 from global tomography, *Nature*, 386(6625), 578.

559 van Keken, P. E., B. R. Hacker, E. M. Syracuse, and G. A. Abers (2011), Subduction factory: 4.
560 Depth-dependent flux of H₂O from subducting slabs worldwide, *Journal of Geophysical*
561 *Research: Solid Earth*, 116(B1).

562 Wadati, K. (1928), Shallow and deep earthquakes, *Geophys. Mag.*, 1, 162-202.

563 Warren, L.M., A. N. Hughes, and P. G. Silver (2007) Earthquake mechanics and deformation in
564 the Tonga-Kermadec subduction zone from fault plane orientations of intermediate- and
565 deep-focus earthquakes. *Journal of Geophysical Research*, 112, 340.

566 Warren, L.M., M.A. Langstaff, and P.G. Silver (2008) Fault plane orientations of intermediate-
567 depth earthquakes in the Middle America Trench. *Journal of Geophysical Research*, 113,
568 19207.

569 Wei, S. S., D. A. Wiens, P. E. van Keken, and C. Cai (2017), Slab temperature controls on the
570 Tonga double seismic zone and slab mantle dehydration, *Science advances*, 3(1), e1601755.

571 Wilkins, S. J., R. A. Schultz, R. C. Anderson, J. M. Dohm, and N. H. Dawers (2002),
572 Deformation rates from faulting at the Tempe Terra extensional province, Mars, *Geophysical*
573 *Research Letters*, 29(18).

574 Worzewski, T., M. Jegen, H. Kopp, H. Brasse, and W. T. Castillo (2011), Magnetotelluric image
575 of the fluid cycle in the Costa Rican subduction zone, *Nature Geoscience*, 4(2), 108.

576 Yamasaki, T., and T. Seno (2003), Double seismic zone and dehydration embrittlement of the
577 subducting slab, *Journal of Geophysical Research: Solid Earth*, 108(B4).

- 578 Zhao, D., Z. Wang, N. Umino, and A. Hasegawa (2007), Tomographic imaging outside a seismic
579 network: Application to the northeast Japan arc, *Bulletin of the Seismological Society of*
580 *America*, 97(4), 1121-1132.
- 581 Zhou, Z., J. Lin, M. D. Behn, and J. A. Olive (2015), Mechanism for normal faulting in the
582 subducting plate at the Mariana Trench, *Geophysical Research Letters*, 42(11), 4309-4317.